



# Amygdalin/chitosan-polyvinyl alcohol/cerium-tannic acid hydrogel as biodegradable long-time implant for cancer recurrence care applications: An *in vitro* study

Fatemeh Hakimi<sup>a,b</sup>, Motahare Sharifyrad<sup>a</sup>, Hajar Safari<sup>c</sup>, Akram khanmohammadi<sup>b</sup>, Sepehr Gohari<sup>a</sup>, Ali Ramazani<sup>b,c,\*</sup>

<sup>a</sup> Student Research Committee, Zanjan University of Medical Sciences, Zanjan, Iran

<sup>b</sup> Department of Pharmaceutical Biomaterials, School of Pharmacy, Zanjan University of Medical Sciences, Zanjan, Iran

<sup>c</sup> Department of Pharmaceutical Biotechnology, School of Pharmacy, Zanjan University of Medical Sciences, Zanjan, Iran

## ARTICLE INFO

### Keywords:

Chitosan  
Polyvinyl alcohol  
Cerium  
Tannic acid  
Amygdalin  
Hydrogel

## ABSTRACT

Cancer recurrence following surgery is a serious and worrying problem for the patient. Common treatment strategies, such as chemotherapy, radiotherapy, and surgery, are restricted because of low uptake of the drugs, poor pharmacokinetic properties, and toxicity issues for healthy tissues. The development of engineering platforms for improving the postoperative treatment of cancer can help solve this problem. In this study, the ceria-tannic acid nanoparticles (CeTA-NPs) were successfully synthesized and characterized. Chitosan-polyvinyl/alcohol (CS-PVA) hydrogels containing CeTA NPs (CS-PVA/CeTA) and amygdalin as an anticancer substance were fabricated using freeze-thaw and immersion-drying techniques. The swelling and degradation behaviors, antibacterial activity, and biocompatibility of as-prepared hydrogel were done. The apoptotic effects of amygdalin/CS-PVA/CeTA hydrogel were evaluated by flow cytometry technique on a human colorectal cancer (SW-480) cell line. The CeTA-NPs were investigated as antibacterial and cross-linker agents for greater stability of the hydrogel network. The CS-PVA/CeTA hydrogel demonstrated good safety and antibacterial activity. The results of swelling and biodegradation suggest that CS-PVA/CeTA hydrogels can inspire long-time application. The anticancer effects of the amygdalin/CS-PVA/CeTA hydrogel were confirmed by apoptosis results. Hence, amygdalin/CS-PVA/CeTA hydrogel can be a promising candidate for long-time biomedical application.

## 1. Introduction

As a complex and challenging disease, cancer is one of the most important causes of mortality worldwide [1,2]. Recent scientific advances have shown that this disease can be treated and controlled despite its high mortality rate. Nevertheless, statistics show that tumor recurrence will still exist in patients several years later, posing a critical challenge in the treatment of cancer [3]. Therefore, many studies are attempting to prevent the recurrence of cancer. Surgery to remove tumor cells is often used as the initial treatment, but the risk of disease comeback because of tumor cells remaining after surgery still exists. Chemotherapy, for reasons including low levels of systemic drug delivery to the primary tumor site, side effects, and the need for frequent injections, is not effective in

\* Corresponding author. Department of Pharmaceutical Biomaterials, School of Pharmacy, Zanjan University of Medical Sciences, Zanjan, Iran.  
E-mail address: [ramazania@zums.ac.ir](mailto:ramazania@zums.ac.ir) (A. Ramazani).

preventing cancer recurrence [4–6]. With the rapid development of new technology such as nanomaterials in recent years, various biomaterials with anticancer activity have been fabricated and studied in *in vitro* and *in vivo* models. To this aim, the microsphere and nanoparticle-based systems were first proposed, the most critical challenges of which are rapid drug release and tumor vessel permeability. Indeed, various nanoparticles can be incorporated with adequate drug molecules to increase stability and enhance pharmacokinetic properties [7–9]. Among various nano-systems, hydrogels are suitable candidates for preparing biodegradable implants because of their unique properties, such as elastic chemical and physical properties, high safety, the controllable release of drugs, and because they mimic biological function [10]. Hence, a hydrogel consisting of chitosan-polyvinyl/ alcohol (CS-PVA) and ceria-tannic acid nanoparticles (CeTA-NPs) incorporated with amygdalin as an anticancer drug were proposed and fabricated in this study. However, the usage of hydrogels faces some challenges, including poor mechanical and stability features, especially for long-term applications. Some strategies can overcome this problem, such as hydrogel modification by cross-linker agents. Various NPs have been reported to modify hydrogels. For example, metal-organic cross-linking in the polymeric network can improve hydrogen bonding [11,12]. Several studies have also reported that polyphenol compounds such as tannic acid (TA) can interact with biomolecules and polymers based on different non-covalent and covalent interactions, including hydrogen, electrostatic and hydrophobic interactions [13,14]. TA is a natural organic compound with broad applicability because of its excellent features, including metal ion chelation, antioxidant and antibacterial activity, and others. Several studies have investigated TA-metal hybrid NPs to prepare drug delivery carriers. Generally, the combination of tannic acid and metal ions has been proposed for biomedicine applications [15–18]. Among the various metals, NPs based on cerium (Ce) metal has demonstrated antibacterial, antioxidant, and anticancer activities in the biomedical field [19,20]. In the current study, CeTA-NPs were investigated as a crosslinker and antibacterial agent to improve the interaction between CS and PVA through hydrogen bonding and ion cross-linking. CS and PVA polymers have many beneficial properties, such as biocompatibility, biodegradability, abundance, immune cell activation, and antimicrobial properties. Reports indicate the wide use of these polymers in tissue engineering, wound dressings, and drug delivery systems [21–24].

Amygdalin is known as a natural anticancer drug because of the presence of a cyanogenic group in its structure [25]. To date, few studies have investigated the administration of amygdalin via nanocarriers [26,27]. The current study investigated the amygdalin/CS-PVA/CeTA hydrogel as an anticancer and antibacterial carrier that induces apoptosis on the SW-480 cell line as well as its biodegradation and biocompatibility properties (Fig. 1). The amygdalin/CS-PVA/CeTA hydrogel is proposed for potential application in cancer recurrence. The current study was approved by the institutional ethical committee of Zanjan University of Medical Sciences (Ethical code: IR. ZUMS.REC.1400.341).

## 2. Materials and methods

### 2.1. Materials

Chitosan ( $M_w \sim 300\text{--}500,000$  dl), polyvinyl alcohol ( $M_w \sim 85,000\text{--}124,000$  dl), cerium nitrate hexahydrate ( $\text{Ce}(\text{NO}_3)_3 \cdot 6\text{H}_2\text{O}$ ), 3-(4, 5-dimethylthiazol-2-yl)-2, 5-diphenyltetrazolium bromide (MTT) dye, tryptic soy broth (TSB), tryptic soy agar (TSA), and tannic acid (TA) amygdalin were purchased from Merck KGaA (Germany). Roswell Park Memorial Institute (RPMI) culture medium, fetal bovine serum (FBS), penicillin-streptomycin, and trypsin-EDTA were obtained from Gibco (USA). Microorganism strains, *Staphylococcus aureus* (*S. aureus*, Gram-positive, ATCC No. 25923) and *Escherichia coli* (*E. coli*, Gram-negative, ATCC No. 25922) were used for antibacterial assay. HEK-293, and SW-480 cell lines were supplied by the Stem Cell Technology Co. (Iran). An annexin V-FITC/PI

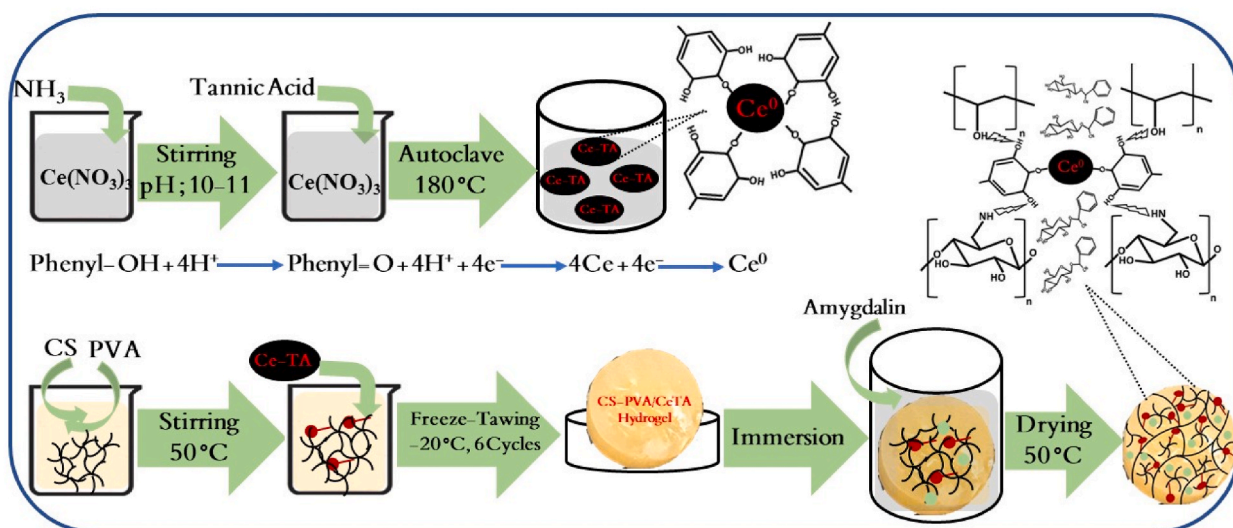


Fig. 1. Schematic of the CeTA NPs and Amygdalin/CS-PVA/CeTA preparation.

apoptosis kit was purchased from Vazyme (Germany).

## 2.2. CeTA-NPs synthesis

In accordance with previous reports, the CeTA-NPs were fabricated by the hydrothermal method [18,28]. Briefly, 500 mg of Ce(NO<sub>3</sub>)<sub>3</sub>·6H<sub>2</sub>O salt was dissolved in 10 ml distilled water under continuous stirring. The NH<sub>3</sub> was added drop by drop in Ce solution to adjust of the pH to 10–11 and afterwards, the solution stirred for 1 h. Then, 100 mg of TA powder was added to the solution, which was the kept in an oven at 180 °C for 12 h. The final precipitation was washed carefully with ethanol, centrifuged at 8000 rpm for 10 min, and then dried for 24 h. After drying, the black powder was obtained as CeTA-NPs.

## 2.3. Preparation of the amygdalin-loaded hydrogel

The hydrogel was prepared in accordance with previous studies with slight modification [29,30]. First, an aqueous PVA solution of 10 % w/w was prepared. Similarly, the CS solution (2 %) was prepared by dissolving the CS powder in acetic acid aqueous solution (70 % w/w). The CS and PVA solutions were mixed in the weight ratio of 50/50 under a magnetic stirrer. Then, 1 mg of CeTA-NPs powder was added to 5 ml of the CS-PVA solution. The mixture was then rapidly stirred with a spatula until homogeneously mixed. Subsequently, the mixture was transferred to a 12-well plate, freeze-thawed at –20 °C for 24 h, and thawed at 25 °C for 1 h. The freeze-thawed method was carried out for six cycles to fabricate the final hydrogel. The as-fabricated hydrogel was immersed in an aqueous-alcoholic (1:1) solution of amygdalin with final concentrations of 1 %, 5 %, and 10 % w/v for 6 h. Finally, the CS-PVA-CeTA and swollen CS-PVA-CeTA hydrogels containing amygdalin drug were dried at 50 °C in an oven for further analyses.

## 2.4. Hydrogel characterization

The morphological properties of the fabricated hydrogel were analyzed using a field emission scanning electron microscope (FE-SEM, MIRA3, Czech) under 20 kV accelerated voltage. A Fourier transform infrared device (FTIR, Tensor 27, Germany) at 400–4000 cm<sup>–1</sup> wavelengths studied the physicochemical and structural properties of the samples, and the optical density of the samples was recorded on a microplate reader spectrophotometer (Tecan, Infinite 200, USA). Apoptosis was investigated by a flow cytometer (BD Biosciences, USA).

## 2.5. Swelling and degradation of the hydrogel

The CS-PVA/CeTA hydrogel was cut into disk shape pieces and weighed ( $W_i$ ) to perform the swelling and degradation tests which were carried out using a phosphate buffered saline (PBS, pH 7.4 and 5.5). Hydrogel samples with the same shape and weight were soaked in 2 ml of PBS solution and incubated at 37 °C under moderate shaking. For the swelling test, the swollen hydrogels were carefully discarded from the PBS (pH 7.4 and 5.5) at specific times (1, 2, 6, 12, 24, 48, and 168 h), gently wiped with soft filter paper, and then weighed ( $W_t$ ). The pre-swollen hydrogels were again soaked in PBS for the next time point of the swelling study. The amount of swelling of the hydrogels was estimated using the following equation (Eq. 1) [31].

$$\text{Swelling (\%)} = \frac{W_t - W_i}{W_i} \times 100 \quad (\text{Eq. 1})$$

The degradation test continued for eight weeks in PBS solution (pH 7.4, 5.5) to examine the stability of the as-fabricated hydrogel and the influence of the as-synthesized CeTA crosslinker. The pre-weighed hydrogel samples ( $W_0$ ) were immersed in PBS and incubated at 37 °C for time intervals of 1, 12, 24, 48, 168, 336, 720, and 1440 h. At the end of every specific time, the hydrogels were removed from the PBS, dried, and weighed ( $W_d$ ). Here, at the pre-mentioned time points, the hydrogel samples were oven-dried at 50 °C until a constant weight ( $W_d$ ) was obtained. The following equation was used to calculate the weight loss of hydrogels (Eq. 2) [32,33].

$$\text{Weight Loss (\%)} = \frac{W_d}{W_0} \times 100 \quad (\text{Eq. 2})$$

The medium was renewed with a fresh solution of PBS every day. The above experiments were carried out in triplicate.

## 2.6. Antibacterial assay

The antibacterial activity of the CS-PVA/CeTA hydrogel was investigated using the agar diffusion test [34,35]. The antibacterial experiment was performed against bacterial strains *S. aureus* and *E. coli*. The bacterial samples were harvested overnight at 37 °C. A swab of harvested bacteria was diluted with broth agar solution after culturing to obtain the standard 0.5 McFarland concentration. Next, 100 µl of diluted bacteria suspension containing ~0.5 McFarland of microorganisms was smeared on the surface of an agar plate. Then, the circular disk of hydrogel was placed onto the surface of the agar plate and incubated at 37 °C for 24 h. A sterilized paper disk served as a negative control. The tests were carried out in triplicate. After incubation, the antibacterial efficiency of the CS-PVA/CeTA hydrogel was calculated by measuring the diameter of the inhibition zone, which is reported as mean ± SD.

## 2.7. Hemocompatibility assay

A blood compatibility test was carried out using an extracted hydrogel liquid. First, 5-mg pieces of CS-PVA/CeTA hydrogel were immersed in 10 ml sterilized PBS solution and maintained at room temperature for 1, 2, and 3 months. After passing the mentioned time intervals, the hydrogels were removed, and the extracted liquid was used for blood compatibility tests performed on blood taken from a healthy volunteer who provided written consent. Then, 200  $\mu$ l of red blood cells (RBCs) with 5 % hematocrit (diluted with sterilized PBS) was added to 800  $\mu$ l of extracted liquid (1, 2, and 3 months) in microtubes and incubated at 37 °C for 2 h. Afterwards, microtubes were centrifuged at 3000 rpm for 5 min. A microplate reader measured the absorbance value (OD) of the supernatant of every sample at 540 nm. Positive and negative control was set by adding 200  $\mu$ l of fresh RBCs (5 % hematocrit) to deionized water and PBS, respectively. The following equation (Eq. 3) was applied to obtain the hemolysis ratio:

$$\text{Hemolysis Ratio(\%)} = \frac{\text{OD of Extract liquid} - \text{OD of Negative Control}}{\text{OD of Positive Control} - \text{OD of Negative Control}} \times 100 \quad (\text{Eq. 3})$$

## 2.8. Cell culture and biocompatibility assay

The HEK-293 cell line was used to investigate the biocompatibility of the prepared hydrogels. The cells were routinely cultured in RPMI 1640 medium enriched with 10 % fetal bovine serum (FBS) and 1 % penicillin-streptomycin solution in culture flasks at 37 °C in 5 % CO<sub>2</sub> for 24 h.

The cytocompatibility and safety of the pre-fabricated hydrogels were evaluated using MTT assay. The dried hydrogel was weighed and dispersed in sterilized PBS to obtain different concentrations (final concentrations were 2, 5, 10, 20, 50, 100, and 200  $\mu$ g/ml). The HEK-293 cells were seeded in 96-well plates at  $2 \times 10^5$  cells/well density. After 24 h incubation at 37 °C, 100  $\mu$ l of the aqueous extract of hydrogels was added to each well and incubation continued for another 24 h. These procedures were performed in triplicate ( $n = 3$ ). After 24 h, the medium was carefully withdrawn, and then, 20  $\mu$ l of MTT solution (5 mg/ml) was added to each cell-hydrogel seeded well. The plates were incubated for a further 4 h, and then 100  $\mu$ l of DMSO solution was added to dissolve the purple formazan crystals. Cells treated with RPMI medium and DMSO solution were used as the negative and positive control, respectively. The absorption values of the formazan solutions were measured at 570 nm on an ELISA microplate reader (Tecan, Infinite 200, USA), and the relative growth rate (RGR) was estimated using the following formula (Eq. 4) [36,37]:

$$\text{RGR (\%)} = \frac{\text{Absorption of Hydrogel samples}}{\text{Absorption of Negative Control}} \times 100 \quad (\text{Eq. 4})$$

## 2.9. Flow cytometry assay

Flow cytometry was assayed on the SW-480 cell line to determine the cytotoxic effect of amygdalin/CS-PVA/CeTA hydrogel involving apoptosis. Annexin V/FITC-PI double staining was done based on the kit protocol of the manufacturer. Briefly, the cells were cultured in 6-well plates and treated with CS-PVA/CeTA and amygdalin/CS-PVA/CeTA hydrogels for 24 h. The treated cells were collected and trypsinized, washed twice with sterilized PBS, and resuspended in a binding buffer. Then they were stained with annexinV/FITC-PI dye and incubated at room temperature for 10 min in the dark. Fluorescence measurements were taken by flow cytometry (BD Bioscience), and data were analyzed by FlowJo software (version V7.6.1) and GraphPad Prism (version 8.0.2).

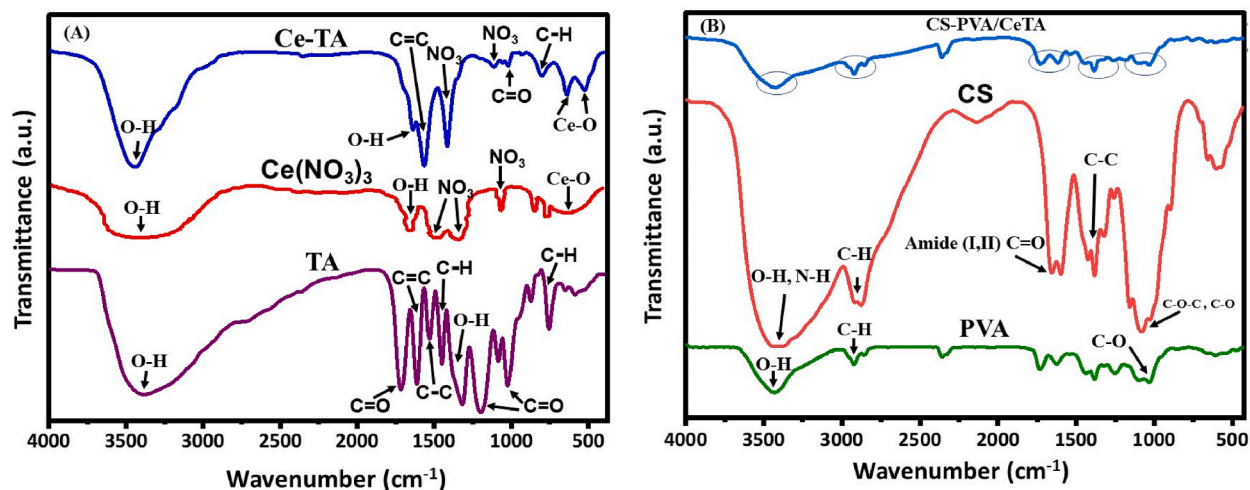


Fig. 2. FTIR spectra of the TA, Ce (NO<sub>3</sub>)<sub>3</sub>, CeTA NPs (A); CS, PVA and CS-PVA/CeTA hydrogel (B).

## 2.10. Statistical analysis

Data were reported as mean  $\pm$  standard deviation. One-way ANOVA was performed to compare the control and treated groups. The differences between the mean of each treated group and control were statistically significant at  $p$ -value  $\leq 0.05$ . Each experiment was repeated at least three times.

## 3. Results and discussion

### 3.1. FTIR study of CeTA NPs

FTIR was used to evaluate interactions and the peak shift in the NPs, and the effects of TA in Ce particles for the preparation of CeTA NPs were also considered. Fig. 2A and B shows the FTIR spectra for all the pure and fabricated materials. All the characteristic peaks of pure CeTA  $(\text{NO}_3)_3$  and CeTA NPs were observed in the FTIR spectrum (Fig. 2A). A hydroxy absorption band at  $3450 \text{ cm}^{-1}$  of both TA and Ce  $(\text{NO}_3)_3$  was visible after CeTA formation. In the CeTA NPs, the band related to the Ce–O stretching became sharper, and one new peak at  $516 \text{ cm}^{-1}$  emerged. The Ce and TA interaction as metal-oxygen caused the band at  $800 \text{ cm}^{-1}$ . Because of the oxidation reaction, the corresponding bands to the phenolic hydroxyl group weakened the FTIR CeTA NPs. The above results confirmed the successful incorporation of TA in the Ce NPs [38,39]. Additionally, the formation of CS-PVA/CeTA hydrogel was confirmed by FTIR spectrum and was depicted in Fig. 2B. In case of pure CS, the absorption peaks appeared around  $1593$ ,  $1655$ , and  $1385 \text{ cm}^{-1}$  are corresponding to bending vibration of the C=O bond (amide I), the N–H bond (amide II) and the distorting vibration of C–CH<sub>3</sub> bond, respectively. The absorption peaks in the range of  $1000$ – $1200 \text{ cm}^{-1}$  are related to C–O–C and C–O stretching. The absorption peaks at  $2920$  and  $2890 \text{ cm}^{-1}$  can be attributed to symmetric and asymmetric stretching of the aliphatic C–H. The broad and strong peak from  $3000$  to  $3700 \text{ cm}^{-1}$  were attributed to symmetric stretching vibration of the O–H and N–H bonds [40,41]. The characteristic peaks of the pure PVA

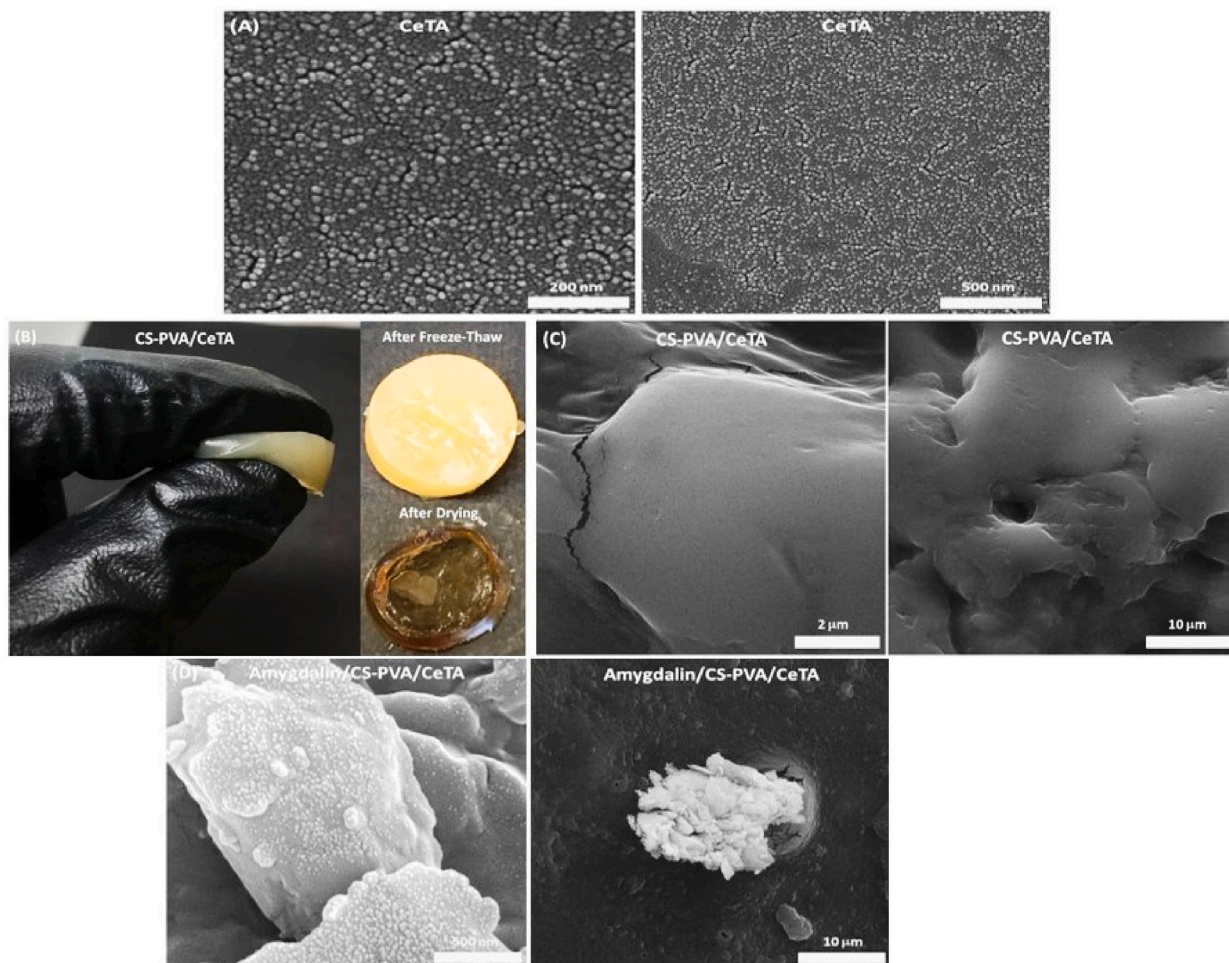


Fig. 3. Macroscopic (B) and microscopic images of the CeTA NPs (A), CS-PVA/CeTA (C) and Amygdalin/CS-PVA/CeTA (D) hydrogels.

appeared at around  $3350\text{ cm}^{-1}$  (O–H stretching),  $2920$  (symmetric  $-\text{CH}_2$ ) and  $1080\text{ cm}^{-1}$  (C–O bond). The FTIR spectra of CS-PVA/CeTA hydrogel showed the major peaks of CS, PVA and CeTA NPs. The characteristics peaks of CeTA NPs at  $1000\text{--}1700\text{ cm}^{-1}$  overlapped with the strong stretching vibration peaks of the CS and PVA. The intensity of the O–H and N–H absorption band at  $3300\text{--}3600\text{ cm}^{-1}$  decreased for the CS-PVA/CeTA hydrogel. These related to the intra-intermolecular hydrogen bonding of O–H and N–H groups. All these changes indicate that the CeTA NPs, CS and PVA chemically compatible and have the intra-intermolecular hydrogen bonding [42,43].

### 3.2. Macroscopic and microscopic studies of CeTA NPs and hydrogel

FE-SEM analysis was used to observe the surface morphology of the NPs and hydrogel. According to Fig. 3A, the CeTA NPs had a spherical shape and a particle size of  $\sim 10\text{ nm}$ . The distribution of particles was uniform. As a reducing agent, TA can reduce cerium ions to metal form and prevent CeTA NPs agglomeration. Fig. 3B shows the macroscopic image of the CS-PVA/CeTA hydrogel. The fabricated hydrogel exhibited a flexible solid structure after freeze-thaw and drying processes. According to Fig. 3C and D, the CS-PVA/CeTA and amygdalin/CS-PVA/CeTA hydrogels showed a relatively smooth and homogenous surface with an integrated porous matrix similar to an extracellular matrix structure. Indeed, crystalline particles with uniform distribution were observed after an immersion-drying process attributed to the incorporation of amygdalin in the hydrogels. The interconnectivity and flexibility of the structure also show that the fabricated hydrogel has good structural stability.

### 3.3. Swelling and degradation studies

Swelling capability and biodegradation rate are vital indicators in evaluating the performance of hydrogels as implantable anti-cancer candidates for the prevention of cancer recurrence [44]. The current study investigated the swelling and biodegradation behavior of the CS-PVA/CeTA hydrogel in PBS (pH 5.5 and 7.4). Greater swelling was obtained in pH 5.5 than pH 7.4 after 6 h, but then it leveled off (Fig. 4A). It seems that  $\text{NH}_2$  groups of CS could swell more under acidic conditions [45–47]. As shown in Fig. 4B, CS-PVA/CeTA hydrogels remained stable for eight weeks in the PBS (pH 5.5 and 7.4) with no weight loss. This observation can be attributed to the hydrolytic stability of fabricated hydrogel. It suggests the biodegradability potential of the hydrogel and its sufficiency in functioning as a drug delivery carrier against tumor cells [48]. Compared with similar hydrogels, CS-PVA/CeTA also exhibited higher structural stability *in vivo* [30,49–51]. These behaviors may be explained by the incorporation of CeTA NPs in the CS-PVA hydrogel. Therefore, the hydrogel was not readily dissociated, and its structure was well preserved. As a result, the CS-PVA/CeTA hydrogel can be used for long-period drug delivery applications, especially for tumor recurrence care.

### 3.4. Antibacterial study of CS-pva/ceta hydrogel

The risk of bacterial infection occurring is a common side effect after surgery or any type of post-treatment of cancer therapy [52]. Recent studies have indicated that the implantation of antimicrobial material into the tumor site could result in anticancer drugs having a more efficient effect. Therefore, the development of antimicrobial carriers plays a crucial role in tumor recurrence treatment. A zone-of-inhibition test evaluated the antibacterial activity of the CS-PVA/CeTA hydrogel. As shown in Fig. 5, the inhibition zone of the CS-PVA/CeTA hydrogel against *S. aureus* (Fig. 5A) and *E. coli* (Fig. 5B) was obtained at about 30 mm. The hydrogel showed good antibacterial properties and thus can be used a drug delivery carrier for cancer therapy.

Furthermore, the fabricated hydrogel is itself active against bacteria. This result shows that the hydrogel carrier consisting of CS-

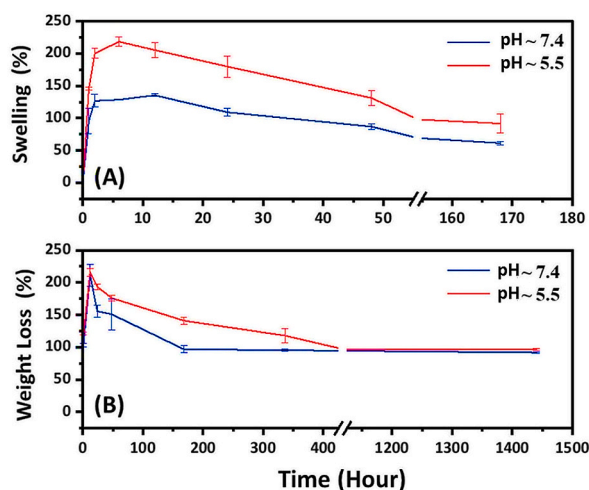
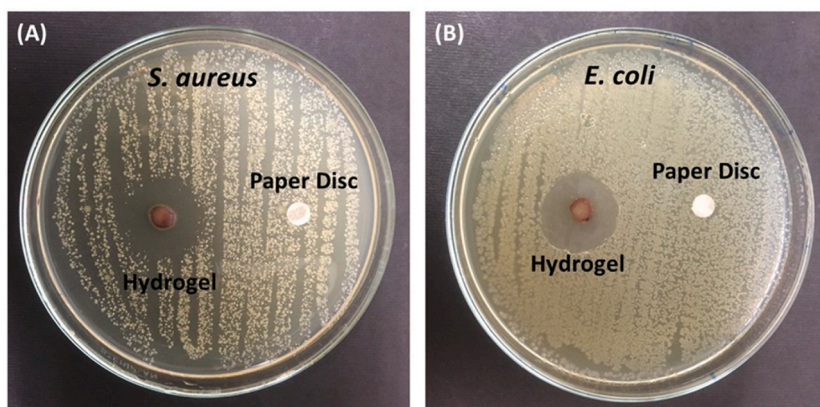


Fig. 4. Degree of swelling (A) and biodegradation (B) of CS-PVA/CeTA hydrogel in PBS at pH 5.5 and 7.4.



**Fig. 5.** Antimicrobial activity of the hydrogels against *S. aureus* (A) and *E. coli* (B). The Zone of inhibition representing the antibacterial effect of CS-PVA/CeTA hydrogel.

PVA and CeTA NPs has excellent antibacterial activity and can be used in cancer recurrence treatment. Moreover, the potent antibacterial ability of the CS-PVA/CeTA hydrogel will enhance the wound healing process after surgery.

### 3.5. Hemocompatibility study of CS-PVA/CeTA hydrogel

Hemocompatibility is an important indicator for exploring the fabricated biomaterial *in vivo*. The lysis of the RBC membrane can result in toxicity of biomaterials at *in vivo* applications [53]. The hemocompatibility result is shown in Fig. 6. A hemolysis ratio of <5% was obtained for all extracted liquids of the CS-PVA/CeTA hydrogel. No significant difference ( $p \geq 0.05$ ) was observed between tested samples in extracted liquids of the CS-PVA/CeTA hydrogel. Therefore, according to the hemotoxicity levels of the ASTM F756-00 standard, the CS-PVA/CeTA formulation is slightly hemolytic [14]. Furthermore, the hemolysis ratios for positive and negative control were 100% and 0%, respectively. These results suggest that the CS-PVA/CeTA hydrogel can be a good candidate for biomedical applications.

### 3.6. Cell viability study of CS-PVA/CeTA hydrogel

Evaluating *in vitro* safety and biocompatibility is vital in toxicology studies of new biomaterials. Cytocompatibility is commonly investigated through cell viability assays [54].

Herein, the cytocompatibility of the hydrogel was conducted using the MTT assay, and the results are presented in Fig. 7. HEK-293 cells were viable at all tested concentrations. According to the United States Pharmacopeia standards, materials with an RGR index of  $\geq 100\%$  are classified as non-cytotoxic levels; between 75% and 99% are slightly cytotoxic and acceptable. In comparison, materials with a RGR  $\leq 74\%$  have remarkable cytotoxic levels [55]. The levels of toxicity were relevant to the nontoxic level of the RGR value at the lower hydrogel concentration of 200  $\mu\text{g}$ . Thus, no cytotoxic components were released from the fabricated hydrogel compared to

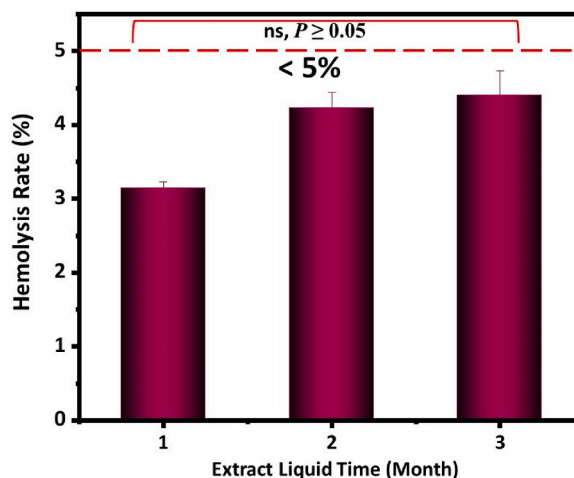


**Fig. 6.** Hemocompatibility of CS-PVA/CeTA hydrogel, ( $P \geq 0.05$ , ns: no significant).

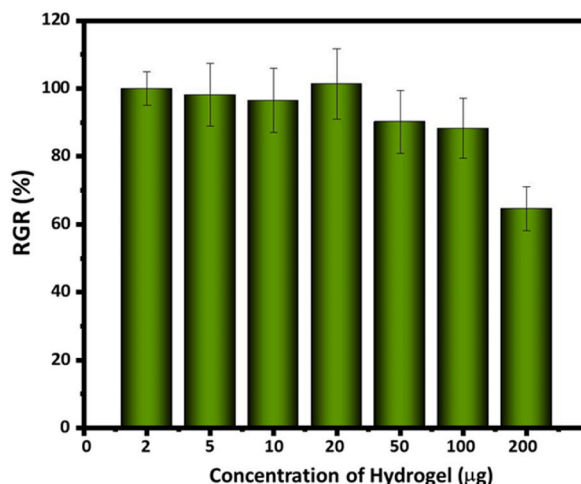


Fig. 7. Cytotoxicity of HEK-293 performed on CS-PVA/CeTA hydrogel after 24 h.

the control on the HEK-293 cell line. The CS-PVA/CeTA hydrogels at 2, 5, 10, 20, 50, and 100 µg/ml were not cytotoxic on healthy cells and thus can be used in the medical applications.

### 3.7. Flow cytometry study

SW-480 cells were treated with CS-PVA/CeTA and amygdalin/CS-PVA/CeTA hydrogels for the flow cytometry experiment. SW-480 cells without hydrogel treatment served as the negative control. The flow cytometry analysis (Fig. 8 A, B, C, D, and E) revealed apoptotic percentages of  $10.24 \pm 0.1271$  %,  $12.67 \pm 0.1140$  %, and  $26.93 \pm 2.330$  % for concentrations of 10, 50, and 100 µg/ml of amygdalin/CS-PVA/CeTA hydrogel, respectively. Moreover, treatment with 100 µg/ml of amygdalin led to more cell apoptosis than lower concentrations. As seen in Fig. 8A, there were no significant apoptotic bodies ( $3.813 \pm 0.4321$ ) when SW-480 cells were treated with 100 µg/ml of CS-PVA/CeTA hydrogel ( $p \leq 0.1032$ ). Fig. 8F shows that treatment of SW-480 cells with amygdalin/CS-PVA/CeTA caused a significant increase in the apoptotic cells in a dose-dependent manner compared to the control group ( $p \leq 0.0008$ ,  $0.0004$ , and  $0.0321$ ). These findings indicate that amygdalin/CS-PVA/CeTA hydrogel could induce apoptotic death in SW-480 cells.

## 4. Conclusion

In conclusion, the amygdalin/CS-PVA/CeTA hydrogel was successfully prepared using a freeze-thaw/immersing-drying process. The stability of hydrogel improved with the addition of CeTA nanoparticles. The prepared hydrogel showed acceptable swelling, biodegradation, anticancer, and antibacterial properties.

The antibacterial effect and safety levels of the CS-PVA/CeTA hydrogel are promising. The swelling and degradation tests revealed that the fabricated CS-PVA/CeTA hydrogel remained stable for 60 days and showed a slow-degrading effect. Flow cytometry analysis revealed that the apoptotic percentage of amygdalin/CS-PVA/CeTA increased significantly from 10 to 100 µg/ml. Overall, the synthesized amygdalin/CS-PVA/CeTA hydrogel seems to be a slow-degrading long-lasting releasing nanocarrier that can potentially be used in the prevention of cancer recurrence.

### Funding statement

This project was supported by research deputy of Zanjan University of Medical Science (ZUMS) for financial support of this project (grant number: A-12-349-45).

### Data availability statement

Data will be made available on request.

### Additional information

No additional information is available for this paper.

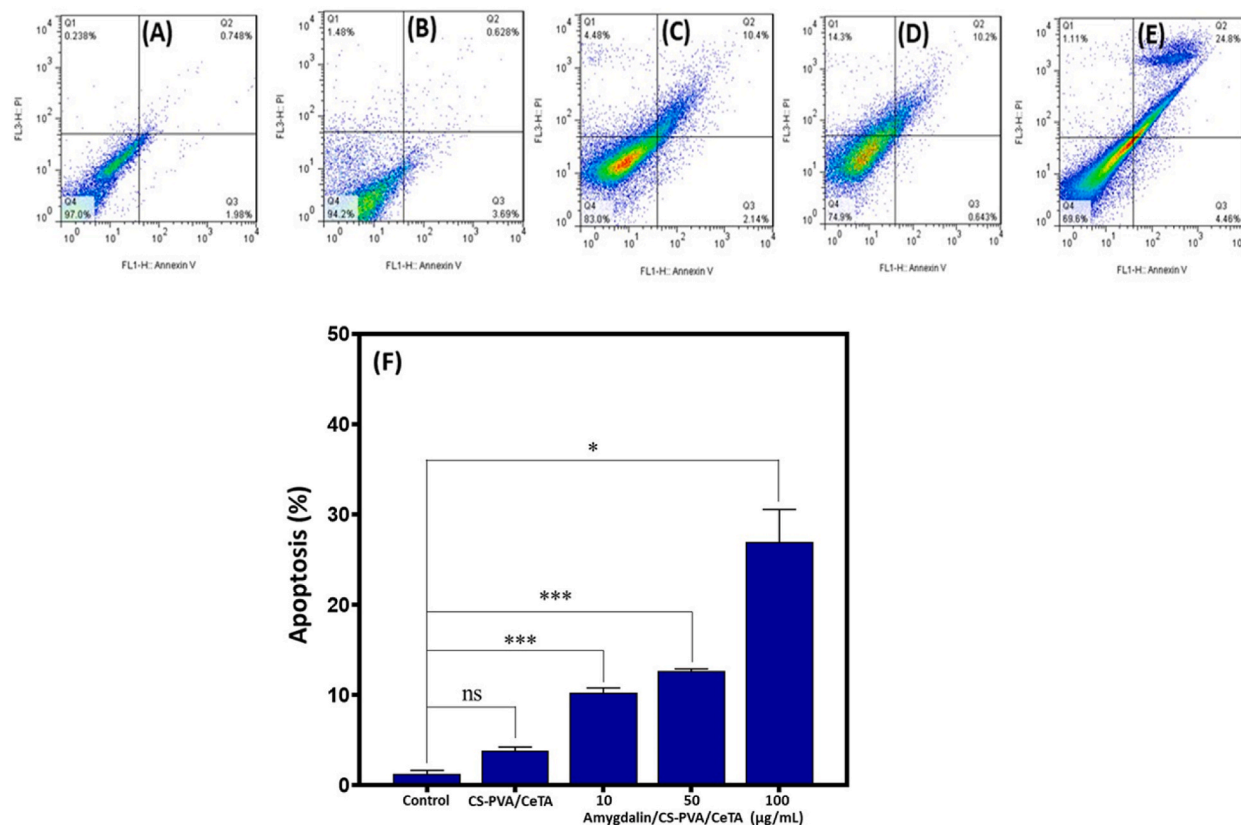


**Fig. 8.** Flow cytometry images of SW-480 cells before (A), after treatment with CS-PVA/CeTA (B) and Amygdalin/CS-PVA/CeTA (C, D, E), Early/Late apoptosis percentages (F) of SW-480 cells before and after treatment with hydrogel for 24 h, (\* $P$ , \*\*\* $P \leq 0.05$ , ns: no significant).

### CRedit authorship contribution statement

**Fatemeh Hakimi:** Data curation, Investigation, Methodology, Writing – original draft. **Motahare Sharifyrad:** Data curation, Methodology. **Hajar Safari:** Data curation, Methodology. **Akram khanmohammadi:** Data curation, Methodology. **Sepehr Gohari:** Methodology. **Ali Ramazani:** Conceptualization, Funding acquisition, Supervision, Writing – review & editing.

### Declaration of competing interest

The authors declare that they have no known competing financial interests or personal relationships that could have appeared to influence the work reported in this paper.

### References

- [1] K. Kalantari, E. Mostafavi, B. Saleh, P. Soltantabar, T.J. Webster, Chitosan/PVA hydrogels incorporated with green synthesized cerium oxide nanoparticles for wound healing applications, *Eur. Polym. J.* 134 (2020), 109853.
- [2] R.L. Siegel, K.D. Miller, A. Jemal, Cancer statistics, 2020, *CA A Cancer J. Clin.* 70 (1) (2020) 7–30.
- [3] H. Phuengkham, C. Song, S.H. Um, Y.T. Lim, Implantable synthetic immune niche for spatiotemporal modulation of tumor-derived immunosuppression and systemic antitumor immunity: postoperative immunotherapy, *Advanced materials (Deerfield Beach, Fla)* 30 (18) (2018), e1706719.
- [4] S. Talebian, J. Foroughi, S.J. Wade, K.L. Vine, A. Dolatshahi-Pirouz, M. Mehrali, et al., Biopolymers for antitumor implantable drug delivery systems: recent advances and future outlook, *Adv. Mater. (Deerfield Beach, Fla)* 30 (31) (2018), e1706665.
- [5] M.J. Esmatabadi, B. Bakhshinejad, F.M. Motlagh, S. Babashah, M. Sadeghizadeh, Therapeutic resistance and cancer recurrence mechanisms: unfolding the story of tumour coming back, *J. Biosci.* 41 (3) (2016) 497–506.
- [6] S. Shen, X. Xu, S. Lin, Y. Zhang, H. Liu, C. Zhang, et al., A nanotherapeutic strategy to overcome chemotherapeutic resistance of cancer stem-like cells, *Nat. Nanotechnol.* 16 (1) (2021) 104–113.
- [7] T. Sun, Y.S. Zhang, B. Pang, D.C. Hyun, M. Yang, Y. Xia, Engineered nanoparticles for drug delivery in cancer therapy, *Angew. Chem.* 53 (46) (2014) 12320–12364.
- [8] Q. Chen, C. Wang, X. Zhang, G. Chen, Q. Hu, H. Li, et al., In situ sprayed bioresponsive immunotherapeutic gel for post-surgical cancer treatment, *Nat. Nanotechnol.* 14 (1) (2019) 89–97.
- [9] A.V. Avgustinovich, O.V. Bakina, S.G. Afanas'ev, O.V. Cheremisina, L.V. Spirina, A.Y. Dobrodeev, et al., Nanoparticles in gastric cancer management, *Curr. Pharmaceut. Des.* 27 (21) (2021) 2436–2444.
- [10] E. Rostami, Progresses in targeted drug delivery systems using chitosan nanoparticles in cancer therapy: a mini-review, *J. Drug Deliv. Sci. Technol.* 58 (2020), 101813.

- [11] H. Shaghholi, S.M. Ghoreishi, M. Mousazadeh, Improvement of interaction between PVA and chitosan via magnetite nanoparticles for drug delivery application, *Int. J. Biol. Macromol.* 78 (2015) 130–136.
- [12] Q. Song, J. Gao, Y. Lin, Z. Zhang, Y. Xiang, Synthesis of cross-linking chitosan-PVA composite hydrogel and adsorption of Cu(II) ions, *Water Sci. Technol. : J. Int. Assoc. Water Pollut. Res.* 81 (5) (2020) 1063–1070.
- [13] C. Jia, D. Cao, S. Ji, X. Zhang, B. Muhoza, Tannic acid-assisted cross-linked nanoparticles as a delivery system of eugenol: the characterization, thermal degradation and antioxidant properties, *Food Hydrocolloids* 104 (2020), 105717.
- [14] B. Kaczmarek, K. Nadolna, A. Owczarek, M. Michalska-Sionkowska, A. Sionkowska, The characterization of thin films based on chitosan and tannic acid mixture for potential applications as wound dressings, *Polym. Test.* 78 (2019), 106007.
- [15] A. Bigham, V. Rahimkhoei, P. Abasian, M. Delfi, J. Naderi, M. Ghomi, et al., Advances in tannic acid-incorporated biomaterials: infection treatment, regenerative medicine, cancer therapy, and biosensing, *Chem. Eng. J.* 432 (2022), 134146.
- [16] M. Krzyżowska, E. Tomaszewska, K. Ranozek-Soliwoda, K. Bień, P. Orłowski, G. Celichowski, et al. (Eds.), *Tannic Acid Modification of Metal Nanoparticles: Possibility for New Antiviral Applications*, 2017.
- [17] P. Orłowski, E. Tomaszewska, K. Ranozek-Soliwoda, M. Gniadek, O. Labeledz, T. Malewski, et al., Tannic Acid-Modified Silver and Gold Nanoparticles as Novel Stimulators of Dendritic Cells Activation, vol. 9, 2018.
- [18] L. Liu, C. Ge, Y. Zhang, W. Ma, X. Su, L. Chen, et al., Tannic acid-modified silver nanoparticles for enhancing anti-biofilm activities and modulating biofilm formation, *Biomater. Sci.* 8 (17) (2020) 4852–4860.
- [19] S. Rajeshkumar, P. Naik, Synthesis and biomedical applications of Cerium oxide nanoparticles – a Review, *Biotechnol. Rep.* 17 (2018) 1–5.
- [20] M. Teng, Z. Li, X. Wu, Z. Zhang, Z. Lu, K. Wu, et al., Development of tannin-bridged cerium oxide microcubes-chitosan cryogel as a multifunctional wound dressing, *Colloids Surf., B* 214 (2022), 112479.
- [21] K. Chandra Hembram, S. Prabha, R. Chandra, B. Ahmed, S. Nimesh, Advances in preparation and characterization of chitosan nanoparticles for therapeutics, *Artif. Cell Nanomed. Biotechnol.* 44 (1) (2016) 305–314.
- [22] T.A. Ahmed, B.M. Aljaeid, Preparation, characterization, and potential application of chitosan, chitosan derivatives, and chitosan metal nanoparticles in pharmaceutical drug delivery, *Drug Des. Dev. Ther.* 10 (2016) 483–507.
- [23] G. Rivera-Hernández, M. Antunes-Ricardo, P. Martínez-Morales, M.L. Sánchez, Polyvinyl alcohol based-drug delivery systems for cancer treatment, *Int. J. Pharm.* 600 (2021), 120478.
- [24] M. Kamaci, İ. Kaya, Biodegradable and antibacterial poly(azomethine-urethane)-chitosan hydrogels for potential drug delivery application 31 (4) (2020) 898–908.
- [25] R. Sohail, S.R. Abbas, Evaluation of amygdalin-loaded alginate-chitosan nanoparticles as biocompatible drug delivery carriers for anticancerous efficacy, *Int. J. Biol. Macromol.* 153 (2020) 36–45.
- [26] S. Senapati, A.K. Mahanta, S. Kumar, P. Maiti, Controlled drug delivery vehicles for cancer treatment and their performance, *Signal Transduct. Targeted Ther.* 3 (1) (2018) 7.
- [27] G. Tiwari, R. Tiwari, B. Sriwastawa, L. Bhati, S. Pandey, P. Pandey, et al., Drug delivery systems: an updated review, *Int. J. Pharmaceut. Invest.* 2 (1) (2012) 2–11.
- [28] M. Mazloum-Ardakani, H. Mohammadian-Sarcheshmeh, H. Naderi, F. Farbod, Sabaghian FijoES, Fabrication of a high-performance hybrid supercapacitor using a modified graphene aerogel/cerium oxide nanoparticle composite, *J. Energy Storage* 26 (2019), 100998.
- [29] K. Kalantari, E. Mostafavi, B. Saleh, P. Soltantabar, T.J. Webster, Chitosan/PVA hydrogels incorporated with green synthesized cerium oxide nanoparticles for wound healing applications, *Eur. Polym. J.* 134 (2020), 109853.
- [30] A. Kumar, T. Behl, S. Chadha, Synthesis of physically crosslinked PVA/Chitosan loaded silver nanoparticles hydrogels with tunable mechanical properties and antibacterial effects, *Int. J. Biol. Macromol.* 149 (2020) 1262–1274.
- [31] K.K. Mahato, I. Yadav, R. Singh, Monika, B.N. Singh, S.K. Singh, et al., Polyvinyl alcohol/chitosan lactate composite hydrogel for controlled drug delivery, *Mater. Res. Express* 6 (11) (2019), 115408.
- [32] X. Hu, Y. Wang, L. Zhang, M. Xu, Formation of self-assembled polyelectrolyte complex hydrogel derived from salectan and chitosan for sustained release of Vitamin C, *Carbohydr. Polym.* 234 (2020), 115920.
- [33] M. Kamaci, İ. Kaya, Chitosan based hybrid hydrogels for drug delivery: preparation, Biodegradation, *Thermal Mech. Prop.* 34 (2) (2023) 779–788.
- [34] Q. Zhu, M. Jiang, Q. Liu, S. Yan, L. Feng, Y. Lan, et al., Enhanced healing activity of burn wound infection by a dextran-HA hydrogel enriched with sanguinarine, *Biomater. Sci.* 6 (9) (2018) 2472–2486.
- [35] V. Vellora Thekkae Padil, N.H. Nguyen, A. Ševcū, Černík MjjoN, Fabrication, characterization, and antibacterial properties of electrospun membrane composed of gum karaya, polyvinyl alcohol, and silver nanoparticles, *J. Nanomater.* 2015 (2015).
- [36] M. Jaiswal, F. Naz, A.K. Dinda, V. Koul, In vitro and in vivo efficacy of doxorubicin loaded biodegradable semi-interpenetrating hydrogel implants of poly (acrylic acid)/gelatin for post surgical tumor treatment, *Biomed. Mater. (Bristol, U. K.)* 8 (4) (2013), 045004.
- [37] S. Bi, J. Pang, L. Huang, M. Sun, X. Cheng, X. Chen, The toughness chitosan-PVA double network hydrogel based on alkali solution system and hydrogen bonding for tissue engineering applications, *Int. J. Biol. Macromol.* 146 (2020) 99–109.
- [38] K.H. Hong, Polyvinyl alcohol/tannic acid hydrogel prepared by a freeze-thawing process for wound dressing applications, *Polym. Bull.* 74 (7) (2017) 2861–2872.
- [39] M. Chelliah, J.B.B. Rayappan, U.M. Krishnan, Synthesis and characterization of cerium oxide nanoparticles by hydroxide mediated approach, *JJoAS, J. Appl. Sci. Res.* 12 (16) (2012) 1734–1737.
- [40] M. Kamaci, İ. Kaya, Fabrication of biodegradable hydrogels based on chitosan and poly(azomethine-urethane) containing phenyl triazine for drug delivery 33 (9) (2022) 2645–2655.
- [41] F. Hakimi, H. Jafari, S. Hashemikia, S. Shabani, A. Ramazani, Chitosan-polyethylene oxide/clay-alginate nanofiber hydrogel scaffold for bone tissue engineering: preparation, physical characterization, and biomimetic mineralization, *Int. J. Biol. Macromol.* 233 (2023), 123453.
- [42] Y.-N. Chen, L. Peng, T. Liu, Y. Wang, S. Shi, H. Wang, Poly(vinyl alcohol)-tannic acid hydrogels with excellent mechanical properties and shape memory behaviors, *ACS Appl. Mater. Interfaces* 8 (40) (2016) 27199–27206.
- [43] T. Li, X. Hu, Q. Zhang, Y. Zhao, P. Wang, X. Wang, et al., Poly(acrylic acid)-chitosan @ tannic acid double-network self-healing hydrogel based on ionic coordination, *Polym. Adv. Technol.* (2020) 31.
- [44] W. Wang, Q. Zhang, M. Zhang, X. Lv, Z. Li, M. Mohammadniaei, et al., A novel biodegradable injectable chitosan hydrogel for overcoming postoperative trauma and combating multiple tumors, *Carbohydr. Polym.* 265 (2021), 118065.
- [45] U. Duru Kamaci, M. Kamaci, Preparation of polyvinyl alcohol, chitosan and polyurethane-based pH-sensitive and biodegradable hydrogels for controlled drug release applications, *JJoPM, Biomaterials P, Int. J. Polym. Mater.* 69 (18) (2020) 1167–1177.
- [46] T. Li, X. Hu, Q. Zhang, Y. Zhao, P. Wang, X. Wang, et al., Poly (acrylic acid)-chitosan@ tannic acid double-network self-healing hydrogel based on ionic coordination, *Polym. Adv. Technol.* 31 (7) (2020) 1648–1660.
- [47] M. Kamaci, İ. Kaya, Preparation of biodegradable, and pH-sensitive poly(azomethine)-chitosan hydrogels for potential application of 5-fluoro uracil delivery, *Eur. Polym. J.* 158 (2021), 110680.
- [48] M.B. Browning, S.N. Cereceres, P.T. Luong, E.M. Cosgriff-Hernandez, Determination of the in vivo degradation mechanism of PEGDA hydrogels, *J. Biomed. Mater. Res., Part A* 102 (12) (2014) 4244–4251.
- [49] K.H. Hong, Preparation and properties of polyvinyl alcohol/tannic acid composite film for topical treatment application, *Fibers Polym.* 17 (12) (2016) 1963–1968.
- [50] Y.-N. Chen, L. Peng, T. Liu, Y. Wang, S. Shi, HJAam Wang, et al., Poly (vinyl alcohol)-tannic acid hydrogels with excellent mechanical properties and shape memory behaviors, *ACS Appl. Mater. Interfaces* 8 (40) (2016) 27199–27206.

- [51] K.K. Mahato, I. Yadav, R. Singh, B.N. Singh, S.K. Singh, B. Ray, et al., Polyvinyl alcohol/chitosan lactate composite hydrogel for controlled drug delivery, *Mater. Res. Express* 6 (11) (2019), 115408.
- [52] D. Tahtat, M. Mahlous, S. Benamer, A. Nacer Khodja, S. Larbi Youcef, N. Hadjarab, et al., Influence of some factors affecting antibacterial activity of PVA/Chitosan based hydrogels synthesized by gamma irradiation, *J. Mater. Sci. Mater. Med.* 22 (11) (2011) 2505–2512.
- [53] M. Nalezinková, In vitro hemocompatibility testing of medical devices, *Thromb. Res.* 195 (2020) 146–150.
- [54] T.L. Riss, R.A. Moravec, A.L. Niles, S. Duellman, H.A. Benink, T.J. Worzella, et al., Cell viability assays, in: S. Markossian, A. Grossman, K. Brimacombe, M. Arkin, D. Auld, C. Austin, et al. (Eds.), *Assay Guidance Manual*, Eli Lilly & Company and the National Center for Advancing Translational Sciences, Bethesda (MD), 2004.
- [55] F. Hakimi, S. Hashemikia, S. Sadighian, A.J.P.B. Ramazani, Nanofibrous chitosan/polyethylene oxide silver/hydroxyapatite/silica composite as a potential biomaterial for local treatment of periodontal disease, *Polym. Bull.* (2022) 1–21.